Int. J. Electron. Commun. (AEÜ) 69 (2015) 1606–1612

Contents lists available at ScienceDirect

International Journal of Electronics and Communications (AEÜ)

journal homepage: www.elsevier.com/locate/aeue

DOA, power and polarization angle estimation using sparse signal reconstruction with a COLD array

Ye Tian*, He Xu

School of Information Science and Technology, Yanshan University, Qinhuangdao, Hebei 066004, China

ARTICLE INFO

Article history:
Received 28 January 2015
Accepted 21 July 2015

Keywords:
Array signal processing
DOA
Power and polarization angle estimation
Sparse signal reconstruction
COLD array

ABSTRACT

Existing polarized source localization methods mostly rely on subspace technique. In this paper, a very different framework, namely sparse signal reconstruction, is extended to estimate direction-of-arrival (DOA), power and polarization angle parameters using a cocentered orthogonal loop and dipole (COLD) array. The key points of the proposed algorithm can be summarized as three aspects: (i) this paper first constructs a special second-order statistics vector by using sum-average arithmetic, which is only the function of DOA and power parameters; (ii) then this paper constructs another three special second-order statistics vectors, which are only the function of polarization parameters; (iii) this paper exploits Zhang penalty to enforce sparsity, which lead to almost unbiased index and amplitude estimation. This paper also demonstrates how to distinguish two sources using their polarization characteristics. Simulation results validate the effectiveness and superiority of the proposed algorithm.

1. Introduction

Direction-of-arrival (DOA) estimation is a key problem in array signal processing fields such as smart antennas, mobile communication systems, radar, sonar, electronic surveillance, and seismic exploration applications [1]. Therefore, it has received a significant amount attention, and various methods have been developed for dealing with this issue, see [2,4,5] and references therein. However, all of them use the array of unpolarized or single polarized scalar sensors, and they do not fully exploit the polarization information embedded in the EM sources.

In the past twenty years, as vector-sensors become more and more reliable, polarization has been added to estimation process as an essential attribute to characterize sources, in addition to their DOAs. Consequently, many methods for DOA and polarization estimation have been developed successively based on different types of arrays [6–11]. Using a single electromagnetic vector sensor, Nehorai et al. [6] developed the vector cross-product DOA estimator, and Wong et al. [7] developed the uni-vector-sensor ESPRIT DOA and polarization estimator. While using a cross-dipole array, Hua et al. [8] and Li et al. [9,10] proposed MUSIC-based and ESPRIT-based DOA and polarization estimators, respectively. In addition, Li et al. [11] also proposed MODE estimator utilizing a cocentered orthogonal loop and dipole (COLD) array, which obtains excellent statistical properties provided that the number of sources is known and a good initialization is given. It should be noted that most of the DOA and polarization estimation methods as mentioned above rely on subspace technique.

Recently, a very different framework, namely sparse signal reconstruction, has been addressed in array signal processing, and many methods including the ℓ_1-norm penalty based methods [12–14], the recursive weighted least-squares FOCUSS method [15] and the $\ell_{2,0}$-norm approximation method [16] are proposed for DOA estimation with scalar sensor arrays. These methods based on sparse signal reconstruction exhibit some advantages, such as high resolution, robustness to noise, and no need to know the prior knowledge of the number of sources. However, all of these methods either require a good initialization or suffer from estimation bias problem. These unresolved issues (especially for the estimation bias problem) restrict the extension of the existing sparse-reconstruction-based methods to polarized array seriously.

In this paper, we propose a novel sparse-reconstruction-based algorithm for DOA, power and polarization angle estimation. Instead of using a single electromagnetic vector sensor and a cross-dipole array, we use a uniform linear COLD array as introduced by Li [11], whose antenna elements are not sensitive to the azimuth angle of the signal. Our aim is to estimate DOA, power and polarization angle parameters from a new framework (i.e., sparse signal reconstruction), and further obtain the performance improvement. To achieve this goal, we first construct several

* Corresponding author. Tel.: +86 335 8057078.
E-mail address: tianye@ysu.edu.cn (Y. Tian).

http://dx.doi.org/10.1016/j.aeue.2015.07.012
1434-8411/

different second-order statistics vectors by utilizing sum-average arithmetic and remove operation, and then exploits Zhang penalty to obtain multi-parameter estimation. Numerical simulations show that the combination of second-order statistics vector model and Zhang penalty can solve the issues emerged in existing sparse-reconstruction-based DOA estimation methods effectively. The proposed algorithm shows the salient advantages, including good robustness to noise (not only suited for suppressing Gaussian white noise, but also suited for suppressing unknown nonuniform noise), not requiring an accurate initialization and no need to know the prior knowledge of the number of sources.

The rest of paper is organized as follows. The polarized far-field signal model with a COLD array is introduced in Section 2. The proposed sparse-reconstruction-based DOA, power and polarization angle estimation algorithm is developed in Section 3. Simulation results are present in Section 4. Conclusions are drawn in Section 5.

2. Polarized far-field signal model

Consider K far-field narrow-band sources impinging on a uniform linear array, which consists of $L=2M+1$ COLD pairs with inter-element spacing Δ. The array configuration is shown in Fig. 1, where all the sensors, namely, $-M, \ldots, 0, \ldots, M$, lie on the y-axis.

Given a completely polarized transverse electromagnetic (TEM) wave propagating into the array, we consider the polarization ellipse produced by its electric field as the incoming wave is viewed from the coordinate origin. The electric field is described as

$$\vec{\mathrm{E}} = E_\theta \vec{\theta} + E_\phi \vec{\Phi} \tag{1}$$

where E_θ is the horizontal component and E_ϕ is the vertical component, and $\vec{\theta}$ and $\vec{\phi}$ are the spherical unit vectors along the azimuth and elevation angles θ and ϕ, respectively. We assume that each dipole in the array is a short dipole with same length and each loop is a small loop with the same area. For a given signal polarization, specified by constants γ and η, the electric-field components are given by

$$E_\theta = E_0 \cos(\gamma),\ E_\phi = E_0 \sin(\gamma) e^{j\eta} \tag{2}$$

where $\gamma \in [0, \pi/2)$ and $\eta \in [-\pi, \pi)$ represent the polarization angle and the polarization phase difference respectively, and are used to characterize the polarization state. E_0 denotes the signal amplitude which is an arbitrary nonzero complex constant. Consequently, the electric-field vector $\vec{\mathrm{E}}$ and the magnetic-field vector $\vec{\mathrm{H}}$ of an incoming signal described by arbitrary electric-field components E_θ and E_ϕ can be written as

$$\vec{\mathrm{E}} = E_\theta \vec{\theta} + E_\phi \vec{\phi} = E_0[\cos(\gamma)\vec{\theta} + \sin(\gamma) e^{j\eta} \vec{\phi}] \tag{3}$$

$$\vec{\mathrm{H}} = Z_0(E_\theta \vec{\phi} - E_\phi \vec{\theta}) = Z_0 E_0[\cos(\gamma)\vec{\phi} - \sin(\gamma) e^{j\eta} \vec{\theta}]. \tag{4}$$

where Z_0 is the transmission mediums intrinsic impedance and is real valued.

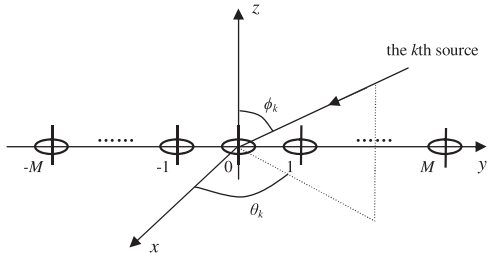

Fig. 1. A uniform linear COLD array.

The main concern of this paper is 1-D DOA estimation (i.e., azimuth angle estimation), which is also a key problem in signal processing fields, see [2–5]. Therefore, we assume that the antennas and the incident signals are coplanar, i.e., $\phi = 90^\circ$. Expressed in Cartesian coordinates after normalization [7], Eqs. (3) and (4) become

$$\vec{\mathrm{E}} = [\cos(\gamma)(-\sin(\theta)\vec{\mathrm{x}} + \cos(\theta)\vec{\mathrm{y}}) - \sin(\gamma) e^{j\eta} \vec{\mathrm{z}}] \tag{5}$$

$$\vec{\mathrm{H}} = [\sin(\gamma) e^{j\eta} (\sin(\theta)\vec{\mathrm{x}} - \cos(\theta)\vec{\mathrm{y}}) - \cos(\gamma)\vec{\mathrm{z}}] \tag{6}$$

with $\vec{\mathrm{x}}$, $\vec{\mathrm{y}}$ and $\vec{\mathrm{z}}$ representing the unit vectors along the x, y and z directions, respectively. Since we utilize the COLD array, the signal components in the $\vec{\mathrm{x}}$ and $\vec{\mathrm{y}}$ directions are eliminated [11]. Therefore, the received signals at sensor m for loop and dipole, denoted by $u_m^{[l]}(t)$ and $u_m^{[d]}(t)$, can be approximated as

$$u_m^{[l]}(t) = -\sum_{k=1}^{K} s_k(t) \cos(\gamma_k) e^{jm\omega_k} + n_m^{[l]}(t) \tag{7}$$

and

$$u_m^{[d]}(t) = -\sum_{k=1}^{K} s_k(t) \sin(\gamma_k) e^{j\eta_k} e^{jm\omega_k} + n_m^{[d]}(t) \tag{8}$$

where $-M \le m \le M$, $s_k(t)$ is the kth source signal, $n_m^{[l]}(t)$ and $n_m^{[d]}(t)$ are the noise components embedded in the mth loop and the mth dipole, respectively. The parameter ω_k is function of the DOA θ_k of the kth source, i.e., $\omega_k = -2\pi\Delta \sin(\theta_k)/\lambda$, where λ is the carrier wavelength.

Let the array center be the phase reference point, the vector form of array output can be written as

$$\mathbf{u}^{[l]}(t) = \mathbf{A}\mathbf{s}^{[l]}(t) + \mathbf{n}^{[l]}(t) \tag{9}$$

and

$$\mathbf{u}^{[d]}(t) = \mathbf{A}\mathbf{s}^{[d]}(t) + \mathbf{n}^{[d]}(t) \tag{10}$$

with

$$\mathbf{u}^{[l]}(t) = [u_{-M}^{[l]}(t), u_{-M+1}^{[l]}(t), \ldots, u_M^{[l]}(t)]^T$$

$$\mathbf{u}^{[d]}(t) = [u_{-M}^{[d]}(t), u_{-M+1}^{[d]}(t), \ldots, u_M^{[d]}(t)]^T$$

$$\mathbf{s}^{[l]}(t) = -[s_1(t)\cos(\gamma_1), \ldots, s_K(t)\cos(\gamma_K)]^T$$

$$\mathbf{s}^{[d]}(t) = -[s_1(t)\sin(\gamma_1) e^{j\eta_1}, \ldots, s_K(t)\cos(\gamma_K) e^{j\eta_K}]^T$$

$$\mathbf{n}^{[l]}(t) = [n_{-M}^{[l]}(t), n_{-M+1}^{[l]}(t), \ldots, n_M^{[l]}(t)]^T$$

$$\mathbf{n}^{[d]}(t) = [n_{-M}^{[d]}(t), n_{-M+1}^{[d]}(t), \ldots, n_M^{[d]}(t)]^T$$

where the superscript T denotes transpose operation. $\mathbf{A} \triangleq [\mathbf{a}(\theta_1), \mathbf{a}(\theta_2), \ldots, \mathbf{a}(\theta_K)]$ is the $L \times K$ steering matrix, whose k column is the $L \times 1$ steering vector corresponding to the DOA of the kth source, i.e., θ_k, and can be expressed as

$$\mathbf{A}(\theta_k) = [e^{-jM\omega_k}, \ldots, 1, \ldots e^{jM\omega_k}]^T. \tag{11}$$

For unique parameter estimation, we make the following assumptions:

[**A1**] The source signals $\{s_1(t), \ldots, s_K(t)\}$ are assumed to be narrow-band, statistically independent processes.

[**A2**] The noise components $\mathbf{n}^{[l]}(t)$, $\mathbf{n}^{[d]}(t)$ are the additive white Gaussian processes or Gaussian unknown nonuniform processes, and independent of the source signals. Meanwhile, the covariance matrices of $\mathbf{n}^{[l]}(t)$, $\mathbf{n}^{[d]}(t)$ are same.

[**A3**] To avoid phase ambiguity problem of parameter estimation, the inter-element spacing of the array is $\Delta \le \lambda/2$. In addition, the number of sources is less than the number of sensors, i.e., $K < L$.

3. The proposed algorithm

3.1. DOA estimation

Second-order statistics is chosen as a key technique for DOA estimation of polarized far-field sources. Using the output data of sensors, we can get the auto-polarized second-order statistics matrices, which are defined as

$$\mathbf{R}_1 = \mathrm{E}\{\mathbf{u}^{[l]}(t)(\mathbf{u}^{[l]}(t))^H\} = \mathbf{A}\mathbf{S}_1\mathbf{A}^H + \mathbf{n} \tag{12}$$

$$\mathbf{R}_2 = \mathrm{E}\{\mathbf{u}^{[d]}(t)(\mathbf{u}^{[d]}(t))^H\} = \mathbf{A}\mathbf{S}_2\mathbf{A}^H + \mathbf{n} \tag{13}$$

where

$$\begin{aligned}\mathbf{S}_1 &= \mathrm{E}\{\mathbf{s}^{[l]}(t)(\mathbf{s}^{[l]}(t))^H\} \\ &= \mathrm{diag}\left\{P_1\cos^2(\gamma_1), \ldots, P_K\cos^2(\gamma_K)\right\}\end{aligned} \tag{14}$$

$$\begin{aligned}\mathbf{S}_2 &= \mathrm{E}\{\mathbf{s}^{[d]}(t)(\mathbf{s}^{[d]}(t))^H\} \\ &= \mathrm{diag}\{P_1\sin^2(\gamma_1), \ldots, P_K\sin^2(\gamma_K)\}\end{aligned} \tag{15}$$

$$\begin{aligned}\mathbf{N} &= \mathrm{E}\{\mathbf{n}^{[l]}(t)(\mathbf{n}^{[l]}(t))^H\} = \mathrm{E}\{\mathbf{n}^{[d]}(t)(\mathbf{n}^{[d]}(t))^H\} \\ &= \mathrm{diag}\{\sigma_1^2, \ldots, \sigma_L^2\}\end{aligned} \tag{16}$$

$(\cdot)^H$ and $\mathrm{E}\{\cdot\}$ denote the conjugate transpose and the expectation operation respectively, and the symbol $\mathrm{diag}\{z_1, z_2\}$ represents a diagonal matrix with diagonal entries z_1 and z_2.

In what follows, it should be stressed that the sensor noise covariances $\sigma_i^2 (1 \le i \le L)$ are identical in the presence of white Gaussian noise, while no longer identical to each other in unknown nonuniform noise scenario.

Using (12) and (13), we can further obtain

$$\begin{aligned}\mathbf{R} &= \mathbf{R}_1 + \mathbf{R}_2 = \mathbf{A}\mathbf{S}\mathbf{A}^H + 2\mathbf{N} \\ &= \sum_{k=1}^{K} P_k \mathbf{a}(\theta_k)\mathbf{a}^H(\theta_k) + 2\mathbf{N}\end{aligned} \tag{17}$$

where $\mathbf{S} = \mathbf{S}_1 + \mathbf{S}_2 = \mathrm{diag}\{P_1, \ldots, P_K\}$. Note that Eq. (17) has the similar form as the array covariance matrix obtained with scalar array, which does not incorporate the signal polarizations. Therefore, it can be regarded that the source signals are completely received.

$\mathbf{R}$ can be expanded as the following form

$$\mathbf{R} = \begin{bmatrix} \sum_{k=1}^{K} P_k + 2\sigma_1^2 & \cdots & \sum_{k=1}^{K} P_k e^{-j(L-1)\omega_k} \\ \vdots & \ddots & \vdots \\ \sum_{k=1}^{K} P_k e^{j(L-1)\omega_k} & \cdots & \sum_{k=1}^{K} P_k + 2\sigma_L^2 \end{bmatrix} \tag{18}$$

It can be easily find that $\mathbf{R}(p, q) = \mathbf{R}(\bar{p}, \bar{q})$ with $p - q = \bar{p} - \bar{q} \neq 0$ regardless of Gaussian white noise or Gaussian unknown nonuniform noise scenarios, where $p, q, \bar{p}, \bar{q} \in [1, L]$. This means that we can provide a better statistical performance model by sum-average arithmetic using $\mathbf{R}$ [17]. For a better estimate, we construct a $4M \times 1$ vector $\mathbf{r}_1$, whose $\tilde{m}$th element is given by

$$\mathbf{r}_1(\tilde{m}) = \begin{cases} \dfrac{1}{\tilde{m}} \displaystyle\sum_{i=1}^{\tilde{m}} \mathbf{R}(i, L + i - \tilde{m}) & \tilde{m} = 1, \ldots, 2M \\ \dfrac{1}{2L - \hat{m}} \displaystyle\sum_{i=1}^{2L-\hat{m}} \mathbf{R}(L + 1 - i, 2L - i - \tilde{m}) & \text{else} \end{cases} \tag{19}$$

with $\hat{m} = \tilde{m} + 1$.

Eq. (19) can be rewritten as

$$\mathbf{r}_1 = \bar{\mathrm{A}}\mathrm{p} \tag{20}$$

where

$$\bar{\mathrm{A}} = [\bar{\mathrm{a}}(\theta_1), \ldots, \bar{\mathrm{a}}(\theta_K)] \tag{21}$$

$$\bar{\mathrm{a}}(\theta_k) = [e^{-j(L-1)\omega_k}, \ldots, e^{-j\omega_k}, e^{j\omega_k}, \ldots, e^{j(L-1)\omega_k}]^T \tag{22}$$

$$\mathbf{p} = [P_1, \ldots, P_K]^T \tag{23}$$

From Eqs. (19) and (20), we can see that $\mathbf{r}_1$ becomes a noise-free model, which means that the noise (Gaussian white noise or Gaussian unknown nonuniform noise) has been suppressed effectively. In fact, the noise-free model $\mathbf{r}_1$, in addition to sum-average arithmetic, is just obtained by a remove operation (i.e., remove the diagonal elements of $\mathbf{R}$). However, it plays an important role in the final performance improvement (see the experiments for details).

Remark 1: If the sensor noise is Gaussian white process and the number of sources is know a prior, the noise covariance can be obtained by maximum likelihood estimate. Then a noise-free model can be obtained by subtracting the noise term. However, when the sensor noise is a Gaussian unknown nonuniform process, the noise variance will be hard to obtain even though the number of sources is known. Fortunately, our adopted remove operation can solve this problem easily.

Remark 2: It should be pointed out that the same strategy (i.e., the combination of sum-average arithmetic and remove operation) has been used in [17], where the array are assumed to be composed of unpolarized or single polarized scalar sensors. However, the difference between the work in [17] and the present work is that the former implement the strategy on scalar array covariance matrix directly, while the latter first construct virtual covariance matrix $\mathbf{R}$ by sum operation using the auto-polarized second-order statistics matrices $\mathbf{R}_1$, $\mathbf{R}_2$, and then implements the strategy on $\mathbf{R}$.

To obtain DOA estimation in sparse signal representation framework, we set $\boldsymbol{\Theta} = \{\bar{\theta}_1, \ldots, \bar{\theta}_Q\}$ be a sampling grid of all potential directions in spatial domain. In general, $Q \gg K$. Consequently, the sparse representation of Eq. (20) can be formulated as

$$\mathbf{r}_1 = \bar{\mathrm{A}}\mathrm{p} = \boldsymbol{\Phi}\bar{\mathrm{p}} \tag{24}$$

where $\boldsymbol{\Phi} = [\bar{\mathrm{a}}(\bar{\theta}_1), \ldots, \bar{\mathrm{a}}(\bar{\theta}_Q)]$, $\bar{\mathrm{p}} = [p_1, \ldots, p_Q]^T$ is a K-sparse vector, whose ith element is nonzero and equal to P_k if source k comes from $\bar{\theta}_i$ and zero otherwise.

Consequently, the DOA and power estimation can be achieved by solving the following optimization problem

$$\min \|\bar{\mathrm{p}}\|_0 \text{ subject to } \mathbf{r}_1 = \boldsymbol{\Phi}\bar{\mathrm{p}} \tag{25}$$

where $\|\cdot\|_0$ denotes ℓ_0-norm. Note that Eq. (25) is nonconvex and non-smooth process and computationally infeasible. An alternative is to use ℓ_1-norm instead of ℓ_0-norm to enforce sparsity, which leads to

$$\min \|\bar{\mathrm{p}}\|_1 \text{ subject to } \mathbf{r}_1 = \boldsymbol{\Phi}\bar{\mathrm{p}} \tag{26}$$

where $\|\cdot\|_1$ denotes ℓ_1-norm.

In fact, we only obtain the estimated result R of $\mathbf{R}$ and r_1 of $\mathbf{r}_1$ according to the limited snapshots of the array output, and they may be approximately equal. Therefore, the optimization problem (26) with constraint can be cast as another kind of unconstrained form given by

$$\min\{\|\mathrm{r}_1 - \boldsymbol{\Phi}\bar{\mathrm{p}}\|_2 + h\|\bar{\mathrm{p}}\|_1\} \tag{27}$$

where $\|\cdot\|_2$ denotes ℓ_2-norm, h is the regularization parameter that controls the tradeoff between ℓ_2-norm term and ℓ_1-norm term.

Formulation (27) can be regarded as a general LASSO problem [18]. However, the direct ℓ_1-norm penalty associated to LASSO have been proven to produce biased estimates, which will penalize larger

coefficients more heavily than smaller coefficients [19,20]. Therefore, we utilize the concept of Zhang penalty [21] to approximate ℓ_0 function and successively obtain good DOA and power estimation. The Zhang penalty can be viewed as a two-stage ℓ_1 penalized optimization problem. The first stage consists firstly in solving a genuine LASSO. Then according to the resulting estimate p and a user-defined threshold τ, the second stage is a weighted LASSO where the weights are

$$\bar{h}_i = \begin{cases} h & \text{if } |\hat{p}_i| \le \tau \\ 0 & \text{otherwise.} \end{cases} \tag{28}$$

The first stage is completed via formulation (27). Sequentially, the optimization problem corresponding to the second stage of Zhang penalty can be formulated as

$$\min\{\|\mathrm{r}_1 - \boldsymbol{\Phi}\bar{\mathrm{p}}\|_2 + h\sum_{i=1}^{Q}|\bar{\mathrm{p}}(i)|I(|\hat{p}_i| \le \tau)\} \tag{29}$$

where the indicator function $I(\cdot)$ is given by

$$I(a \le b) = \begin{cases} 1, & \text{if } a \le b \\ 0, & \text{otherwise.} \end{cases} \tag{30}$$

In practical applications, the parameter τ must be tuned such that $0 < \tau < \min\{\mathrm{p}(\bar{i})\}, \bar{i} \in X_0$, to make the approximation error of the Zhang penalty to the ℓ_0 function become zero, where X_0 denotes the support of nonzero elements or K larger elements in p.

As stated in [21], the two-stage LASSO of Zhang penalty can lead to a good approximation of ℓ_0-function, and the corresponding estimator is unbiased, which means that we can obtain a good estimation result of $\bar{\mathrm{p}}$. Let p' be the final estimation result of (29), then the DOA and power parameters can be obtained by finding the indexes and amplitudes of nonzero coefficients in p', respectively.

3.2. Polarization angle estimation

To obtain polarization angle estimation, we first obtain cross-polarized second-order statistics matrix $\mathbf{R}_3$, i.e.,

$$\mathbf{R}_3 = \mathrm{E}\{\mathbf{u}^{[l]}(t)(\mathbf{u}^{[d]}(t))^H\} = \mathbf{A}\mathbf{S}_3\mathbf{A}^H \tag{31}$$

where

$$\begin{aligned}\mathbf{S}_3 &= \mathrm{E}\{\mathbf{s}^{[l]}(t)(\mathbf{s}^{[d]}(t))^H\} \\ &= \mathrm{diag}\{P_1\cos(\gamma_1)\sin(\gamma_1)e^{-j\eta_1}, \ldots, . \\ &\qquad P_K\cos(\gamma_K)\sin(\gamma_K)e^{-j\eta_K}\}\end{aligned} \tag{32}$$

Similar to the way as described in Eq. (19), we construct another two $4M \times 1$ vectors $\mathbf{r}_2$, $\mathbf{r}_3$ using $\mathbf{R}_1$, $\mathbf{R}_2$ and one $(4M+1) \times 1$ vector $\mathbf{r}_4$ using $\mathbf{R}_3$ by sum-average arithmetic, which are expressed as

$$\mathbf{r}_2 = \bar{\mathrm{A}}\mathbf{p}_1 \tag{33}$$

$$\mathbf{r}_3 = \bar{\mathrm{A}}\mathbf{p}_2 \tag{34}$$

$$\mathbf{r}_4 = \mathbf{A}\mathbf{p}_3 \tag{35}$$

where

$$\mathbf{p}_1 = [P_1\cos^2(\gamma_1), \ldots, P_K\cos^2(\gamma_K)]^T \tag{36}$$

$$\mathbf{p}_2 = [P_1\sin^2(\gamma_1), \ldots, P_K\sin^2(\gamma_K)]^T \tag{37}$$

$$\begin{aligned}\mathbf{p}_3 = [&P_1\cos(\gamma_1)\sin(\gamma_1)e^{-j\eta_1}, \ldots, \\ &P_K\cos(\gamma_K)\sin(\gamma_K)e^{-j\eta_K}]^T\end{aligned} \tag{38}$$

The sparse representation of Eqs. (33)–(35) are

$$\mathbf{r}_2 = \bar{\mathrm{A}}\mathbf{p}_1 = \Phi\bar{\mathrm{p}}_1 \tag{39}$$

$$\mathbf{r}_3 = \bar{\mathrm{A}}\mathbf{p}_2 = \Phi\bar{\mathrm{p}}_2 \tag{40}$$

$$\mathbf{r}_4 = \mathbf{A}\mathbf{p}_3 = \boldsymbol{\Phi}'\bar{\mathrm{p}}_3 \tag{41}$$

where $\boldsymbol{\Phi}' = [\mathbf{a}(\bar{\theta}_1), \ldots, \mathbf{a}(\bar{\theta}_Q)]$, $\bar{\mathrm{p}}_1 \sim \bar{\mathrm{p}}_3$ are the K-sparse vectors, whose ith element are nonzero and equal to $P_k\cos^2(\gamma_k)$, $P_k\sin^2(\gamma_k)$ and $P_k\cos(\gamma_k)\sin(\gamma_k)e^{-j\eta_k}$ respectively, if source signal k comes from $\bar{\theta}_i$ for some k and zero otherwise. Obviously, we can obtain the polarization angle estimation if $\bar{\mathrm{p}}_\kappa$ is constructed, where $\kappa \in \{1, 2, 3\}$. To avoid estimation bias problem, here we also use Zhang penalty to enforce sparsity. That is, the initial estimation is obtained via LASSO, and the optimization problem corresponding to the second stage are formulated as

$$\min\left\{\|\mathrm{r}_2 - \boldsymbol{\Phi}\bar{\mathrm{p}}_1\|_2 + h\sum_{i=1}^{Q}|\bar{\mathrm{p}}_1(i)|I(|\hat{p}_{1,i}| \le \tau_1)\right\} \tag{42}$$

$$\min\left\{\|\mathrm{r}_3 - \boldsymbol{\Phi}\bar{\mathrm{p}}_2\|_2 + h\sum_{i=1}^{Q}|\bar{\mathrm{p}}_2(i)|I(|\hat{p}_{2,i}| \le \tau_2)\right\} \tag{43}$$

$$\min\left\{\|\mathrm{r}_4 - \boldsymbol{\Phi}'\bar{\mathrm{p}}_3\|_2 + h\sum_{i=1}^{Q}|\bar{\mathrm{p}}_3(i)|I(|\hat{p}_{3,i}| \le \tau_3)\right\} \tag{44}$$

where $\hat{p}_{\kappa,i}$ denotes the ith element of the initial estimation result p_κ, r_κ is the estimated result of $\mathbf{r}_\kappa$. A large number of simulations suggest that $\tau_\kappa = 0.99 \times \min\{\mathrm{p}_\kappa(\bar{i})\}(\bar{i} \in X_0)$ is a good choice for -15 dB$\sim$15 dB SNR.

Define p'_κ be the final estimation results of Eqs. (42)–(44), then the polarization angle can be estimated by

$$\hat{\gamma}_k = [\arctan(|\mathrm{p}'_3(\hbar)|/\mathrm{p}'_1(\hbar)) + \arctan(\mathrm{p}'_2(\hbar)/|\mathrm{p}'_3(\hbar)|)]/2 \tag{45}$$

where $k \in [1, K]$, $\hbar$ is the index of the kth nonzero element in p_κ.

Theorem 1: Let P_1, P_2 denote the power of the first and the second source signals, respectively. Define $\rho_\hbar = \mathrm{p}'_1(\hbar)\mathrm{p}'_2(\hbar) - |\mathrm{p}'_3(\hbar)|^2$, if only one source signal impinging on the array from θ, then $\rho_\hbar = 0$. In contrast, if two source signals impinging on the array from same θ, while the polarized parameter γ_1 and γ_2 are different, then $\rho_\hbar \ge P_1P_2\sin^2(\gamma_2 - \gamma_1) > 0$.

Proof: If only one source signal impinging on the array from θ with power P, we must have

$$\rho_\hbar = P^2|\cos^2(\gamma)\sin^2(\gamma) - |\cos(\gamma)\sin(\gamma)e^{-j\eta}|^2| = 0 \tag{46}$$

In contrast, if two source signals impinging on the array with same θ, the parameter $\rho_\hbar$ can be given by

$$\begin{aligned}\rho_\hbar &= [(P_1\cos^2(\gamma_1) + P_2\cos^2(\gamma_2))(P_1\sin^2(\gamma_1) + P_2\sin^2(\gamma_2)) \\ &\quad -|P_1\cos(\gamma_1)\sin(\gamma_1)e^{-j\eta_1} + P_2\cos(\gamma_2)\sin(\gamma_2)e^{-j\eta_2}|^2] \\ &\ge [(P_1\cos^2(\gamma_1) + P_2\cos^2(\gamma_2))(P_1\sin^2(\gamma_1) + P_2\sin^2(\gamma_2)) \\ &\quad -(P_1\cos(\gamma_1)\sin(\gamma_1) + P_2\cos(\gamma_2)\sin(\gamma_2))^2] \\ &= P_1P_2(\cos(\gamma_1)\sin(\gamma_2) - \cos(\gamma_2)\sin(\gamma_1))^2 \\ &= P_1P_2\sin^2(\gamma_2 - \gamma_1)\end{aligned} \tag{47}$$

Note that $\gamma \in [0, \pi/2)$, if the polarization angles γ_1 and γ_2 are different, i.e., $\gamma_1 \ne \gamma_2$, then $\gamma_2 - \gamma_1 \in (-\pi/2, 0) \cup (0, \pi/2)$, therefore $\rho_\hbar \ge P_1P_2\sin^2(\gamma_2 - \gamma_1) > 0$.

Remark 3: Theorem 1 indicates that the proposed algorithm can identify two sources with same DOA successfully, provided that the polarization angles are different, and the identification performance becomes better with $\gamma_1 \to \pi/2$, $\gamma_2 \to 0$ or $\gamma_2 \to \pi/2$, $\gamma_1 \to 0$.

The regularization parameter h plays an important role in the final performance, where a large value may cause wrong source parameters estimation, while a small value may produce many spurious peaks. Our experimental results suggest that $h = 1$ is a good

choice for 0–15 dB SNR. While in low SNR cases, we use leave-one-out cross-validation [22,23] to select it properly. We divide the data r_1 into $4M$ equal parts including training set and validation set. For each set $g = 1, 2, \ldots, 4M$, fit the model with parameter h to the other $4M-1$ parts, giving p_g and compute its error in predicting the gth part, then the cross-validation error is given by

$$e(h) = \frac{1}{4M}\sum_{g=1}^{4M} \|r_1^g - \boldsymbol{\Phi}^g p_g(h)\|_2^2 \tag{48}$$

where r_1^g, $\boldsymbol{\Phi}^g$ are the gth part of r_1 and $\boldsymbol{\Phi}$, respectively. Repeat this operation for some values of h around 1 and select the value of h that makes $e(h)$ smallest.

3.3. Description of the proposed algorithm

The proposed algorithm can be described as follows:

Step 1: Construct $r_1 \sim r_4$ by sum-average arithmetic, such as the way described in (19);

Step 2: Utilize genuine LASSO to provide the initial estimates p of $\bar{p}$ and p_κ of $\bar{p}_\kappa$, $\kappa \in \{1, 2, 3\}$;

Step 3: Set $\tau_\kappa = 0.99 \times \min\{p_\kappa(\bar{i})\}(\bar{i} \in X_0)$, and successively obtain the final estimation results p' and p'_κ from (29), (42)–(44), respectively.

Step 4: Obtain DOA and power parameters by finding the indexes and amplitudes of nonzero coefficients in p';

Step 5: Obtain polarization angle estimation from (45);

Step 6: Judge if there exist two sources impinging on array from same DOA via parameter $\rho_{\hbar}$.

In fact, if the initial estimates p of $\bar{p}$ and p_κ of $\bar{p}_\kappa$ is not provided by LASSO, but fixed to be $\mathbf{0}$, then the two-stage LASSO is converted into genuine LASSO. This means that the global minimum of the proposed algorithm is still guaranteed without the need for an accurate initialization. Meanwhile, since the proposed algorithm is not relying on the structural assumptions of the orthogonality of the signal and noise subspace, therefore, it can estimate DOAs without knowing the prior knowledge of the number of sources.

3.4. Computational complexity analysis

Regarding the computational complexity, we consider the major part. The calculation of $\mathbf{R}_1 \sim \mathbf{R}_3$ requires $O(L^2\tilde{N})$, where $\tilde{N}$ denotes the snapshot number. Implementing one sparse signal reconstruction or one cross-validation requires $O(Q^3)$. Typically assuming $K < L \ll Q$, therefore the computational complexity of the proposed algorithm is mainly in sparse signal reconstruction and cross-validation process, and is somewhat higher than the ESPRIT-Like method [9] and the MODE method [11], where the main complexity is in calculating the array covariance matrix and its eigenvalue decomposition (the multiplication required is $O(L^2\tilde{N}) + O(L^3)$). However, it should be stressed that the proposed algorithm can provide an improved performance.

4. Simulations

In this section, some experiments are conducted to assess the proposed algorithm. A 7-element linear uniform COLD array with element spacing $\Delta = \lambda/2$ is considered. The sensor noise is Gaussian white process except for the second experiment and the signal power is equal except for the last experiment. The ESPRIT-Like method with cross-dipole array [9], the MODE method with COLD array [11] and Cramér-Rao lower bound (CRLB) are selected as the compared methods. In the simulations, we first divide direction domain into 181 grids from -90° to 90° with 1° interval, and then set a finer grid around the estimated DOAs by exploiting the adaptive grid refinement strategy [12]. The root mean square error (RMSE) that indicates the performance of the proposed algorithm is obtained by 500 independent Monte Carlo trails.

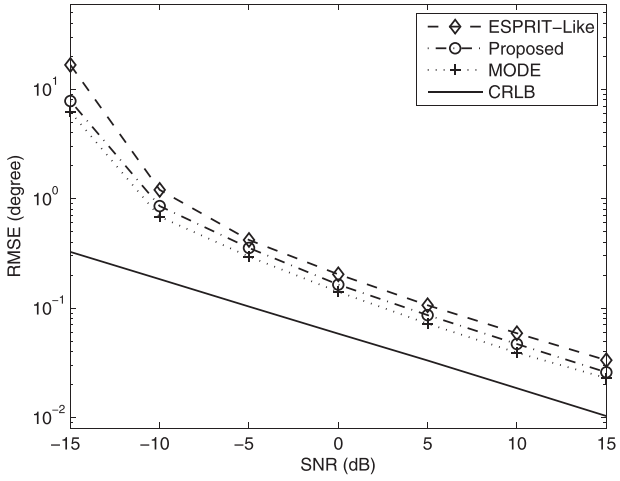

Fig. 2. RMSE of the DOA estimations versus SNR with 500 snapshots in Gaussian white noise.

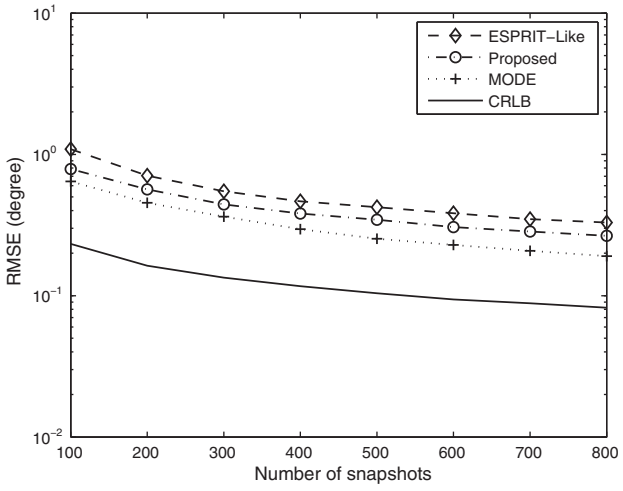

Fig. 3. RMSE of the DOA estimations versus the number snapshots with −5 dB SNR in Gaussian white noise.

In the first experiment, we compare the RMSE of the DOA estimations versus SNR and the number of snapshots in Gaussian white noise, whose curves are plotted in Figs. 2 and 3, respectively. Two sources located at $\theta_1 = -45^\circ$, $\theta_2 = 30^\circ$ are considered, and the corresponding polarization parameters (γ, η) are $(20^\circ, 0^\circ)$ and $(60^\circ, 0^\circ)$. As shown in Figs. 2 and 3, the proposed algorithm outperforms the ESPRIT-Like method in the whole SNR and snapshots regions, but slightly under-performs the MODE method. This phenomenon can be explained as follows. For DOA estimation, the proposed algorithm only use part (auto-polarized data) of the array output, so that the performance is reduced in some degrees. However, it should be noted that the proposed algorithm can estimate DOAs without an accurate initialization.

In the second experiment, we compare the RMSE of the DOA estimations versus SNR and the number of snapshots in Gaussian unknown nonuniform noise, whose curves are plotted in Figs. 4 and 5, respectively. The simulation condition is similar to the first experiment expect that the noise covariance matrix is nonuniform, and has the following form

$$\mathbf{N} = \mathrm{diag}[1.0\ 0.5\ 0.2\ 5.0\ 2.0\ 1.6\ 3.1] \tag{49}$$

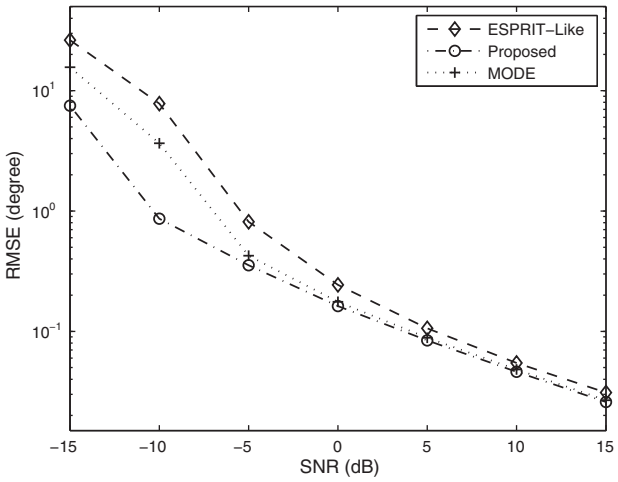

Fig. 4. RMSE of the DOA estimations versus SNR with 500 snapshots in Gaussian unknown nonuniform noise.

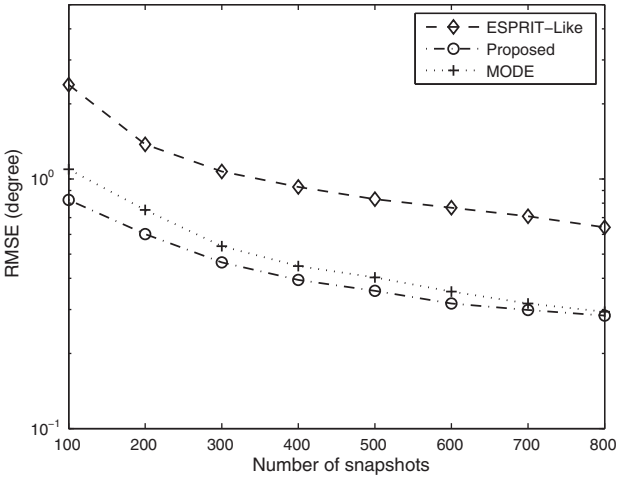

Fig. 5. RMSE of the DOA estimations versus the number snapshots with −5 dB SNR in Gaussian unknown nonuniform noise.

From Figs. 4 and 5, we can see that the proposed algorithm outperforms the compared methods, and the RMSE curve decreases monotonically with the number of snapshots. This confirms that the proposed algorithm is better suited for dealing with unknown nonuniform noise compared with the existing polarized DOA estimation methods.

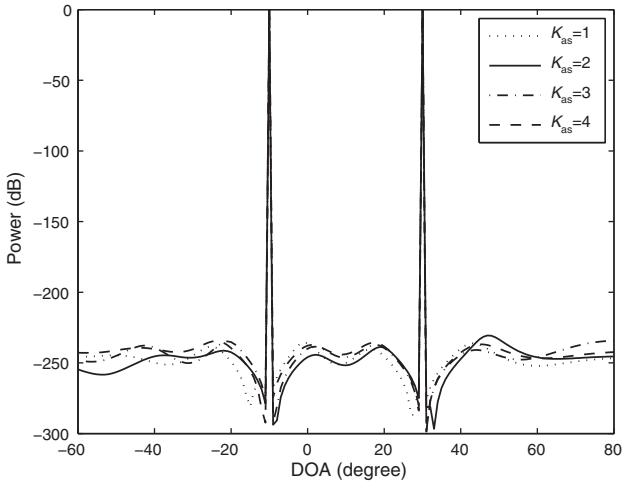

Fig. 6. Sensitivity of the proposed algorithm to the assumed number of sources with 10 dB SNR and 500 snapshots.

In the third experiment, we show the sensitivity of the proposed algorithm to the wrong determination of the number of sources. The actual number of sources is $K=2$, and the assumed number of sources K_{as} varies from 1 to 4. The SNR and the number of snapshots are fixed at 10 dB and 500, respectively. $\theta_1=-10^\circ$, $\theta_2=30^\circ$, polarization parameters are same with the first experiment. The spatial spectrum output is shown in Fig. 6, which demonstrates that the proposed algorithm can provide better robustness to the wrong determination of the number of sources. As stated in Sections 3–3.3, this phenomenon can be explained that we are neither relying on the structural assumptions of the orthogonality of the signal and noise subspace nor implementing singular value decomposition (SVD) on array data.

In the fourth experiment, the SNR, the number of snapshots are fixed at 15 dB and 1000 respectively, the signal power of two sources are set to be $P_1=0.8$, $P_2=1$. Two different cases of source signals incident are considered: (i) the DOAs of two signals are different, whereas the polarization angles are same, i.e., $\{\theta_1=-10^\circ, \gamma_1=20^\circ, \eta_1=0^\circ\}$, $\{\theta_2=30^\circ, \gamma_2=20^\circ, \eta_2=0^\circ\}$. (ii) the polarization angles of two signals are different, whereas the DOAs are same, i.e., $\{\theta_1=-10^\circ, \gamma_1=20^\circ, \eta_1=0^\circ\}$, $\{\theta_2=-10^\circ, \gamma_2=60^\circ, \eta_2=0^\circ\}$. The simulation results are shown in Fig. 7(a) and (b), respectively. From the simulation results, we can easily observe that the proposed algorithm can identify two sources effectively if their DOAs are different. In particular, if two sources impinging on the array with same DOA, while the polarization angles are different, see Fig. 7(b),

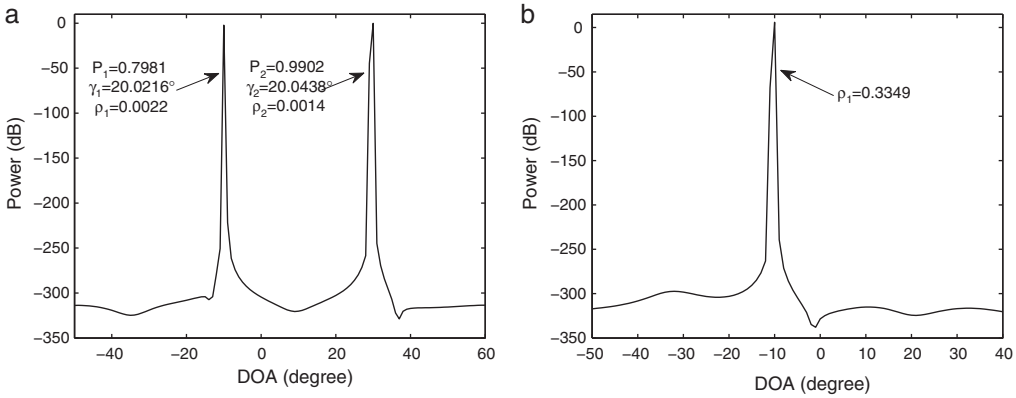

Fig. 7. Spatial spectrum obtained by the proposed algorithm with 15 dB SNR and 1000 snapshots, $P_1=0.8$, $P_2=1$. (a) $\{\theta_1=-10^\circ, \gamma_1=20^\circ, \eta_1=0^\circ\}$, $\{\theta_2=30^\circ, \gamma_2=20^\circ, \eta_2=0^\circ\}$. (b) $\{\theta_1=-10^\circ, \gamma_1=20^\circ, \eta_1=0^\circ\}$, $\{\theta_2=-10^\circ, \gamma_2=60^\circ, \eta_2=0^\circ\}$.

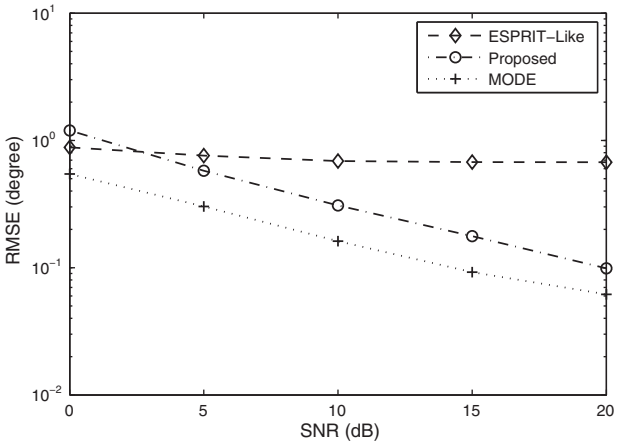

Fig. 8. RMSE of the polarization angle estimations versus SNR with 500 snapshots.

we obtain $\rho_1 = 0.3349$ by calculation, which means that the proposed algorithm can identify them successfully. Moreover, if only one source signal impinging on the array from θ_k or $\rho_k = 0$, we can also obtain a good power and polarization angle estimation.

In the last experiment, we further compare the RMSE of the polarization angle estimations versus SNR. The number of snapshots is fixed at 500, and the polarization parameters are same with the first experiment. Given the fact that polarization estimation performance of the ESPRIT-Like method is influenced by the incident angle seriously (see Fig. 5 of reference [9]), we set the DOAs of two sources to be $\theta_1 = -10^\circ$, $\theta_2 = 10^\circ$, respectively. As shown in Fig. 8, the proposed algorithm outperforms the ESPRIT-Like method when SNR>0 dB, but under-performs the MODE method. The main reason leading to this result is that we use part data of the array output, as well as amplitude estimation strategy. However, it is just because of the amplitude estimation strategy we adopted, the proposed algorithm can distinguish two sources with same DOA easily.

5. Conclusion

In this paper, we have addressed how the multiple parameters of polarized far-field sources can be exactly obtained in sparse signal reconstruction framework using a linear uniform COLD array. In the specific scheme, we first construct several special vectors by sum-average arithmetic using auto-polarized and cross-polarized second-order statistics matrices, then exploit Zhang penalty to enforce sparsity and successively obtain a good DOA, power and polarization angle estimation. We also demonstrate how to distinguish two sources using their polarization characteristics. Finally, we exam the performance of the proposed algorithm by numerical simulations, and illustrate that the proposed algorithm holds several superiorities compared with existing subspace-based polarized far-field source localization methods.

Acknowledgement

The author would like to thank anonymous reviewers for their valuable comments and suggestions. This paper is supported by the National Nature Science Foundation of China (Grant No: 61471313), Doctoral Foundation of Yanshan University (Grant No: B887) and Youth Foundation of Yanshan University (Grant No: 14LGA012).

References

[1] Krim H, Viberg M. Two decades of array signal processing research: the parameter approach. IEEE Trans Signal Process Mag 1996;13:67–94.
[2] Schmidt RO. Multiple emitter location and signal parameter estimation. IEEE Trans Antennas Propag 1986;34:276–80.
[3] Roy R, Kailath T. ESPRIT-estimation of signal parameters via rotational invariance techniques. IEEE Trans Acoust Speech Signal Process 1989;37:984–95.
[4] Li J, Zhang X. Unitary subspace-based method for angle estimation in bistatic MIMO radar. Circuit Syst Signal Process 2014;33:501–13.
[5] Qiao C, Huang L, So HC. Computationally efficient ESPRIT algorithm for direction-of-arrival estimation based on Nyström method. Signal Process 2014;94:74–80.
[6] Nehorai A, Paldi E. Vector-sensor array processing for electro-magnetic source localization. IEEE Trans Signal Process 1994;42:376–98.
[7] Wang KT, Zoltowski MD. Uni-vector-sensor ESPRIT for multisource azimuth, elevation, and polarization estimation. IEEE Trans Antennas Propag 1997;45:1467–74.
[8] Hua Y. A pencil-MUSIC algorithm for finding two-dimensional angles and polarization using cross dipoles. IEEE Trans Antennas Propag 1993;41:370–6.
[9] Li J, Compton Jr RT. Angle and polarization estimation using ESPRIT with a polarization sensitive array. IEEE Trans Antennas Propag 1991;39:1376–83.
[10] Li J, Compton Jr RT. Angle estimation using a polarization sensitive array. IEEE Trans Antennas Propag 1991;39:1539–43.
[11] Li J, Stoica P, Zheng D. Efficient direction and polarization estimation with a COLD array. IEEE Trans Antennas Propag 1996;44:539–47.
[12] Malioutov D, Cetin M, Willsky AS. A sparse signal reconstruction perspective for source localization with sensor arrays. IEEE Trans Signal Process 2005;53:3010–22.
[13] Zheng C, Li G, Zhang H, Wang X. An approach of DOA estimation using noise subspace weighted ℓ_1 minimization. In: Proc. 2011 IEEE Int Conf Acoust Speech and Signal Process (ICASSP). 2011. p. 2856–9.
[14] Yin J, Chen T. Direction-of-arrival estimation using a sparse representation of array covariance vectors. IEEE Trans Signal Process 2011;59:4489–93.
[15] Gorodnitsky IF, Rao BD. Sparse signal reconstruction from limited data using FOCUSS: a re-weighted minimum norm algorithm. IEEE Trans Signal Process 1997;45:600–16.
[16] Hyder MM, Mahata K. Direction-of-arrival estimation using a mixed $\ell_{2,0}$ norm approximation. IEEE Trans Signal Process 2010;58:4646–55.
[17] Tian Y, Sun X. DOA estimation in the presence of unknown nonuniform noise without knowing the number of sources. Int J Electron Lett 2014:1–9 [ahead-of-print].
[18] Tibshirani R. Regression shrinkage and selection via the lasso. J R Stat Soc Ser B 1996;58:267–88.
[19] Fan J, Li R. Variable selection via nonconcave penalized likelihood and its oracle properties. J Am Stat Assoc 2001;96:1348–60.
[20] Gasso G, Rakotomamonjy A, Canu S. Recovering sparse signals with a certain family of non-convex penalties and DC programming. IEEE Trans Signal Process 2009;57:4686–98.
[21] Zhang T. Some sharp performance bounds for least squares regression with ℓ_1 regularization. Ann Stat 2009;37:2109–44.
[22] Shao J. Linear model selection by cross-validation. J Am Stat Assoc 1993;88:486–94.
[23] Kohavi R. A study of cross-validation and bootstrap for accuracy estimation and model selection. In: Proc the 14th International Conf Artificial Intell San Mateo, CA. Los Altos, CA: Morgan Kaufmann; 1995. p. 1137–43.